Quantum correlated pulses from a synchronously pumped optical parametric oscillator operating above threshold

Valentin A. Averchenko, Yuri M. Golubev
V. A. Fock Physics Institute, St. Petersburg State University
198504 St. Petersburg, Stary Petershof, ul. Ul'yanovskaya, 1, Russia

Claude Fabre, Nicolas Treps
Laboratoire Kastler Brossel, Université Pierre et Marie Curie-Paris6,
Place Jussieu, CC74, 75252 Paris Cedex 05, France
(Dated: January 19, 2013)

We perform the quantum analysis of the light emitted by a synchronously pumped optical parametric oscillator operating in the above threshold regime, i.e. when the peak power of pulsed pumping exceeds the threshold of continuous generation. We show that both regimes (below and above threshold) are realized at different times within each pulse of the signal field. We show that the quantum fluctuations of signal and pump pulses are correlated between nearby pulses at times that are placed in the same position relative to the center of the pulses, whereas fluctuations are totally not correlated at different times within the same pulse. The model also predicts the existence of cross-correlations between pump and signal pulses.

It is shown theoretically that there is suppression of quantum noise at the frequencies multiple of the pulse repetition frequency in the spectra of phase quadratures of pump and signal fields measured by a balanced homodyne detection with a pulsed local oscillator.

PACS numbers: 42.50.Dv, 42.50.Yj, 42.65.Re

I. INTRODUCTION

Development and investigation of effective sources of non-classical multimode light are among current trends of quantum optics [1–3]. These sources appear as a main component required for parallel quantum information protocols [4, 5]. From this point of view an optical parametric oscillator (OPO) pumped by a mode-locked laser with a period of pulses which is equal to the round-trip time of the oscillator cavity (so called synchronously pumped OPO or SPOPO [6]) looks quite promising. A modal approach used in [7, 8] showed that quantum state of signal light of a SPOPO operating below threshold in a degenerate regime generates a tensor product of squeezed states in different super-modes, each being a particular coherent superposition of longitudinal modes of different frequencies. Therefore the signal light generated by a SPOPO appears as an interesting resource for parallel quantum information protocols such as quantum teleportation and quantum key distribution.

The same system was also considered in the time domain [9] using a simple physical model that neglects all dispersion effects in the parametric crystal. It was shown in particular that the quantum fluctuations of signal field are not correlated at different times within each individual pulse whereas they are correlated between nearby pulses at times that are placed in the same position relative to the center of the pulses. This paper dealt with the SPOPO operating below threshold. However it is well known that the light of a continuously pumped OPO also reveals nonclassical properties above the oscillation threshold. [10]. Therefore the question about the quantum properties of SPOPO light above threshold looks quite natural.

In the paper [11] it was predicted that a multimode OPO (i.e. which is simultaneously resonant for several spatial or temporal modes) above threshold generates bright light in a single mode whereas the other modes stay in noncritically squeezed vacuum states, i.e. the amount of squeezing does not depend on threshold excess. The prediction was confirmed by an experiment on parametric generation of TEM_{10} and TEM_{01} modes in squeezed vacuum states when the threshold is crossed. In our case it is interesting to check this prediction for the SPOPO, which is another multimode system.

In this paper we will analyze the above threshold behaviour of SPOPO in the time domain where the system operation is described by two coupled equations for envelopes of pump and signal pulses. The physical model and the two-time technique used to describe the field evolution inside the oscillator cavity are similar to the ones applied in [9] for the analysis of the below threshold regime.

The paper is organized as follows. In Sec. II we present our model of SPOPO and write Heisenberg-Langevin equations that describe in time domain its operation above the oscillation threshold. In Sec. III we estimate classical steady-state envelopes of generated pump and signal pulses. We assume that the pump pulses of oscillator have a rectangular shape. We determine quantum fluctuations of fields around the steady-state values in Sec. IV. For this purpose we solve linearized Heisenberg-Langevin equations applying adiabatic elimination of the pump field. As a

result we calculate and analyze pair correlation functions for the quadrature components of the output pulses. In the Sec. VI we consider the model of balanced homodyne detection of pulsed field and calculate the spectra of the photocurrent fluctuations. We generalize the results obtained for rectangular pump and local oscillator pulses to the case of arbitrary envelopes of pulses.

II. PHYSICAL MODEL AND MAIN EQUATIONS

A quantum analysis of the SPOPO below threshold on the basis of time approach has been performed in [9]. As a result two-time correlation functions were obtained for the output signal field which correspond to the following picture of the system operation. Under pulsed laser pumping of a $\chi^{(2)}$ nonlinear crystal (see Fig. 1), placed inside a ring optical cavity of the oscillator, pump photons are parametrically down-converted into pairs of correlated signal photons. The photons of each pair may leave the cavity in different pulses, during an overall time of the order of photon lifetime in a cavity κ_s^{-1}, giving rise to temporal correlations on the same range of time difference. Approximations of thin nonlinear crystal and instantaneous down-conversion, used in the work, lead to the peculiarity that field fluctuations at different times in a single pulse are not correlated.

We will consider SPOPO operation above oscillation threshold on the basis of the physical model that we have used in the below threshold situation. Similarly we assume a degenerate parametric interaction for the carrier frequencies of the pump and signal modes, meaning that the following phase matching condition is fulfilled $\Delta k = k_p(\omega_p) - 2k_s(\omega_p/2) = 0$, where $k_p(\omega_p)$ and $k_s(\omega_p/2)$ are wave vectors of carriers of pump and signal fields. The SPOPO ring cavity is resonant and of high-finesse both for pump and signal fields, so that the doubly-resonant configuration is realized. It takes the same time T_R for pump and signal pulses to make a single round trip inside the cavity and this time is equal to the pump repetition rate. We assume also that the cavity is dispersion-compensated by intracavity dispersive elements. This implies that optical pulses of arbitrary shapes are not distorted after one round trip inside the cavity.

The above threshold regime is achieved by increasing the pump power. In this regime pump depletion becomes significant as well as the process of up-conversion of pairs of signal photons into pump photons. Under these conditions the system becomes nonlinear. In particular one can expect that correlations between the pump and signal pulses will develop. Therefore an adequate system description must consider the coupled evolutions of both fields.

In order to describe system operation we use the time-domain approach presented in detail in Appendix A. The Heisenberg-Langevin equations obtained under this approach have the following form [9]

$$\frac{\partial \hat{A}_p(t,T)}{\partial T} = -\kappa_p \left(\hat{A}_p(t,T) - A_0(t) \right) - g\hat{A}_s^{\,2}(t,T) + \hat{F}_p(t,T), \tag{1}$$

$$\frac{\partial \hat{A}_s(t,T)}{\partial T} = -\kappa_s \hat{A}_s(t,T) + 2g\hat{A}_p(t,T)\hat{A}_s^\dagger(t,T) + \hat{F}_s(t,T) \tag{2}$$

Here $\hat{A}_p(t,T)$ and $\hat{A}_s(t,T)$ are quantized envelopes of pump and signal pulses inside the cavity. Time argument t is treated as the time deviation from the pulse center and it changes in the interval from $-T_R/2$ to $T_R/2$; the dependence of envelopes on the second time argument T describes their changes from pulse to pulse. The amplitudes are normalized so that values $\langle \hat{A}_{p,s}^\dagger \hat{A}_{p,s} \rangle$ have the meaning of mean fluxes in photons per second through the cross sections of the light beams. κ_p and κ_s are the loss rates of pump and signal fields respectively; g is a constant characterizing the parametric coupling; $A_0(t)$ is the classical steady-state envelope of the pump pulses inside the cavity, depending only on time t since the pump pulses are supposed to be perfectly identical. One can write this envelope in the following general form

$$A_0(t) = \sqrt{N_0(t)}\, e^{i\phi_{in}(t)}, \tag{3}$$

where $N_0(t)$ is the intensity shape of the pump pulses and $\phi_{in}(t)$ their possible phase modulation.

The last terms in equations $\hat{F}_p$ and $\hat{F}_s$ describe Langevin noise sources which are related to the vacuum fluctuations of the incoming fields. In this case the fields have zero mean values and characterized by the following nonzero pair correlation functions (for details see Appendix B)

$$\langle \hat{F}_r(t,T)\hat{F}_r^\dagger(t',T')\rangle = 2\kappa_r\, \delta(T-T')\delta(t-t'), \qquad r = s,p \tag{4}$$

III. OSCILLATION THRESHOLD AND SEMICLASSICAL STEADY-STATE SOLUTIONS

As it is known (see, for example, [10]), an optical parametric oscillator is a system that exhibits properties of a second-order phase transition when pump power achieves a certain threshold value. In our notation the threshold

power reads

$$N_{th} \equiv \frac{\kappa_s^2}{4g^2}. \tag{5}$$

For pulsed pumping the threshold is achieved when the peak power of pulses is equal to this value. Evidently, corresponding mean power can be much less than the threshold value. This is an important advantage of pulsed pumping with respect to the continuous one.

It is important to note that in the Heisenberg-Langevin equations (1) and (2) time t appears as a parameter and the Langevin noise sources are delta-correlated relative to this time according to (4). Hence in our model different temporal parts of an individual pulse (pump or signal one) develop in time T independently of other parts with corresponding instantaneous value of the external pump power $N_0(t)$. As a result both regimes (below and above threshold) could be realized within the single pulse at different time instants if peak pump power exceeds threshold value (see Fig. 2). This situation is analogous to what happens in the spatial domain in a degenerate confocal cavity[12]. Since the properties of pulsed fields below threshold were analyzed in [9] we will consider further the simplest case, when external pump pulses have rectangular temporal shape of duration τ_p with intensity exceeding threshold one. In the last section we will generalize our results to arbitrary envelopes of the pulses.

Let us define a time dependent pump parameter:

$$\mu(t) \equiv \sqrt{\frac{N_0(t)}{N_{th}}} \tag{6}$$

For rectangular pump pulses the parameter is non-zero $\mu_0 > 1$ when t changes from $-\tau_p/2$ to $\tau_p/2$. Between pump pulses the generated fields are vacuum noise while within the pulses they develop in a way that is described by coupled Heisenberg-Langevin equations. At this time intervals the fields are characterized by non zero average amplitudes. Here we determine the average steady-state amplitudes denoted as A_p and A_s. In the next section we will analyze the properties of the fluctuations around the average The amplitudes must satisfy equations which are the classical counterparts of Heisenberg-Langevin equations (1) and (2). Technically, we replace the operator quantities in these equations by the c-number quantities and to reject the noise sources. Finally setting partial derivatives equal to zero, we find the stationary solutions in the form

$$A_p(t) = \sqrt{N_p}\, e^{i\phi_{in}(t)}, \qquad A_s(t) = \pm\sqrt{N_s}\, e^{i\phi_{in}(t)/2} \tag{7}$$

Classical intensities N_p and N_s are defined by the following expressions

$$N_p = N_{th}, \quad N_s = \frac{2\kappa_p}{\kappa_s}\,(\mu_0 - 1)N_{th}, \tag{8}$$

which agree with the fact that the average amplitude of pumping field inside the cavity (and respectively at the output) does not depend on the pump intensity[13]. Also one can see that there are two possible opposite phases of the signal field for a fixed pump phase. One can show that both solutions are stable [10].

IV. SOLUTIONS OF LINEARIZED HEISENBERG-LANGEVIN EQUATIONS

The following expressions define the quantum fluctuations of envelopes of pump $\delta\hat{A}_p$ and signal $\delta\hat{A}_s$ fields within the pulses (i.e. at time interval $-\tau_p/2 \le t \le \tau_p/2$)

$$\hat{A}_p(t,T) = (\sqrt{N_p} + \delta\hat{A}_p(t,T))e^{i\phi_{in}(t)}, \tag{9}$$

$$\hat{A}_s(t,T) = (\pm\sqrt{N_s} + \delta\hat{A}_s(t,T))e^{i\phi_{in}(t)/2} \tag{10}$$

Let us assume that the fluctuations are small compared to the mean values

$$\delta\hat{A}_r(t,T) \ll \sqrt{N_r}, \qquad r = p, s \tag{11}$$

It will be shown later that above threshold these inequalities are well-satisfied. Substituting expressions (9) and (10) into (1) and (2) and ignoring the second-order terms according to the assumption of small fluctuations, one obtains the following linearized equations for the fluctuations of fields

$$\frac{\partial}{\partial T}\delta\hat{A}_p(t,T) = -\kappa_p\delta\hat{A}_p(t,T) \mp 2g\sqrt{N_s}\,\delta\hat{A}_s(t,T) + \hat{F}_p(t,T), \tag{12}$$

$$\frac{\partial}{\partial T}\delta\hat{A}_s(t,T) = -\kappa_s\delta\hat{A}_s(t,T) + 2g\sqrt{N_p}\,\delta\hat{A}_s^\dagger(t,T) \pm 2g\sqrt{N_s}\,\delta\hat{A}_p(t,T) + \hat{F}_s(t,T) \tag{13}$$

These equations can be conveniently solved by writing them in terms of quadrature components of fields defined as real and imaginary parts of complex amplitudes:

$$\delta\hat{A}_r(t,T) = \delta\hat{X}_r(t,T) + i\delta\hat{Y}_r(t,T), \tag{14}$$

where $\delta\hat{X}_r = \delta\hat{X}_r^\dagger$ and $\delta\hat{Y}_r = \delta\hat{Y}_r^\dagger$. This choice of quadrature components is such that their fluctuations define fluctuations of intensities and phases of fields, respectively. These quadrature components can be experimentally measured using balanced homodyne detection of fields under appropriate choice of the local oscillator field that will be considered in the Sec. VI.

One gets the following equations for quadrature components of pumping field

$$\frac{\partial}{\partial T}\delta\hat{X}_p(t,T) = -\kappa_p\delta\hat{X}_p(t,T) \mp 2g\sqrt{N_s}\,\delta\hat{X}_s(t,T) + \hat{F}_p'(t,T), \tag{15}$$

$$\frac{\partial}{\partial T}\delta\hat{Y}_p(t,T) = -\kappa_p\delta\hat{Y}_p(t,T) \mp 2g\sqrt{N_s}\,\delta\hat{Y}_s(t,T) + \hat{F}_p''(t,T), \tag{16}$$

and signal field

$$\frac{\partial}{\partial T}\delta\hat{X}_s(t,T) = \pm 2g\sqrt{N_s}\,\delta\hat{X}_p(t,T) + \hat{F}_s'(t,T), \tag{17}$$

$$\frac{\partial}{\partial T}\delta\hat{Y}_s(t,T) = -2\kappa_s\delta\hat{Y}_s(t,T) \pm 2g\sqrt{N_s}\,\delta\hat{Y}_p(t,T) + \hat{F}_s''(t,T) \tag{18}$$

Here we took into account that above threshold $N_p = \kappa_s^2/(4g^2)$ and we also defined hermitian quadrature components of Langevin sources:

$$\hat{F}_p(t,T)e^{-i\phi_{in}} = \hat{F}_p'(t,T) + i\hat{F}_p''(t,T), \tag{19}$$

$$\hat{F}_s(t,T)e^{-i\phi_{in}/2} = \hat{F}_s'(t,T) + i\hat{F}_s''(t,T), \tag{20}$$

with the following correlation functions, obtained from (4):

$$\langle\hat{F}_r'(t,T)\hat{F}_r'(t',T')\rangle = \langle\hat{F}_r''(t,T)\hat{F}_r''(t',T')\rangle = \frac{\kappa_r}{2}\,\delta(T-T')\delta(t-t'), \tag{21}$$

$$\langle\hat{F}_r'(t,T)\hat{F}_r''(t',T')\rangle = -\langle\hat{F}_r''(t,T)\hat{F}_r'(t',T')\rangle = i\frac{\kappa_r}{2}\,\delta(T-T')\delta(t-t') \tag{22}$$

Expression (22) shows that the quadratures of fields are correlated. Thus fluctuations of X- and Y-quadratures of pump and signal fields will be also correlated. Nevertheless in the case we are interested in these correlations are not important.

Let us consider the case when relaxation of the pump field in the cavity with the rate κ_p is the fastest process. Then equations (15)-(18) can be solved using adiabatic elimination of this field. Setting derivatives equal to zero in equations (15)-(16), the fluctuations of the pump field have the form

$$\begin{pmatrix}\delta\hat{X}_p(t,T)\\ \delta\hat{Y}_p(t,T)\end{pmatrix} = \mp\sqrt{\frac{\kappa_x}{\kappa_p}}\begin{pmatrix}\delta\hat{X}_s(t,T)\\ \delta\hat{Y}_s(t,T)\end{pmatrix} + \frac{1}{\kappa_p}\begin{pmatrix}\hat{F}_p'(t,T)\\ \hat{F}_p''(t,T)\end{pmatrix} \tag{23}$$

Inserting these expressions into equations (17) and (18), one gets simple differential equations which have the following solutions

$$\begin{pmatrix}\delta\hat{X}_s(t,T)\\ \delta\hat{Y}_s(t,T)\end{pmatrix} = \int_{-\infty}^{T} dT'\left[\pm\sqrt{\frac{\kappa_x}{\kappa_p}}\begin{pmatrix}\hat{F}_p'(t,T')\\ \hat{F}_p''(t,T')\end{pmatrix} + \begin{pmatrix}\hat{F}_s'(t,T)\\ \hat{F}_s''(t,T)\end{pmatrix}\right]e^{-\kappa_{x,y}(T-T')}, \tag{24}$$

where $\kappa_x = 2\kappa_s(\mu_0 - 1)$ and $\kappa_y = 2\kappa_s\mu_0$ are effective damping rates of fluctuations. According to adiabatic approximation these rates fulfill the condition $\kappa_x, \kappa_y \ll \kappa_p$ that limits pump parameter $\mu_0 \ll \kappa_p/\kappa_s$. We will show further that the main quantum effects appear close to the oscillation threshold when $\mu_0 \approx 1$, which is in agreement with our restriction.

These solutions enable us to determine the properties of the output fields which are of practical interest. For this purpose one uses the boundary condition on the output mirror that reads

$$\hat{A}_r^{out}(t,T) = \sqrt{\mathcal{T}_r}\hat{A}_r(t,T) - \sqrt{1-\mathcal{T}_r}\hat{A}_r^{in}(t,T). \tag{25}$$

Here $\mathcal{T}_r$ is the transmission coefficient of the cavity mirror related to the loss rate of the field $\kappa_r = \mathcal{T}_r/(2T_R)$ (when $\mathcal{T}_r \ll 1$). Also vacuum fluctuations of the incoming field $\hat{A}_r^{in}$ in the expression are related to Langevin noise sources $\hat{F}_r$ according to (B1). The boundary condition is also valid for the quadrature components of fields.

V. CORRELATIONS BETWEEN PULSES

Let us now determine the correlation functions of the quadratures of output fields. Before it we turn from time t that describes a deviation from center of pulses to usual time scale. For this one returns to the discrete pulse numbering, replacing time T with discrete number n and time t with $t - nT_R$ in the following way:

$$\begin{aligned} &T \to nT_R, \quad t \to t - nT_R, \quad T_R\delta(T - T') \to \delta_{nn'}, \\ &\delta\hat{X}_r^{out}(t,T) \to \delta\hat{X}_{r,n}^{out}(t - nT_R), \quad \delta\hat{Y}_r^{out}(t,T) \to \delta\hat{Y}_{r,n}^{out}(t - nT_R). \end{aligned} \tag{26}$$

Thus, using results of the previous section, we obtain the following pair correlation for the quadrature components of pump pulses

$$\langle \delta\hat{X}_{p,n}^{out}(t - nT_R)\delta\hat{X}_{p,n'}^{out}(t' - n'T_R)\rangle = \frac{1}{4}\left(\delta_{nn'}\delta(t-t') + 2\kappa_s T_R e^{-2\kappa_s T_R(\mu_0 - 1)|n-n'|}\delta(t - t' - (n-n')T_R)\right), \tag{27}$$

$$\langle \delta\hat{Y}_{p,n}^{out}(t - nT_R)\delta\hat{Y}_{p,n'}^{out}(t' - n'T_R)\rangle = \frac{1}{4}\left(\delta_{nn'}\delta(t-t') - 2\kappa_s T_R \frac{(\mu_0 - 1)}{\mu_0} e^{-2\kappa_s T_R\mu_0|n-n'|}\delta(t - t' - (n-n')T_R)\right) \tag{28}$$

and signal pulses

$$\langle \delta\hat{X}_{s,n}^{out}(t - nT_R)\delta\hat{X}_{s,n'}^{out}(t' - n'T_R)\rangle = \frac{1}{4}\left(\delta_{nn'}\delta(t-t') + \frac{\kappa_s T_R}{\mu_0 - 1} e^{-2\kappa_s T_R(\mu_0 - 1)|n-n'|}\delta(t - t' - (n-n')T_R)\right), \tag{29}$$

$$\langle \delta\hat{Y}_{s,n}^{out}(t - nT_R)\delta\hat{Y}_{s,n'}^{out}(t' - n'T_R)\rangle = \frac{1}{4}\left(\delta_{nn'}\delta(t-t') - \frac{\kappa_s T_R}{\mu_0} e^{-2\kappa_s T_R\mu_0|n-n'|}\delta(t - t' - (n-n')T_R)\right). \tag{30}$$

These expressions are similar to the correlation functions of pulsed signal field generated by SPOPO below oscillation threshold. The first terms on the right hand side which are proportional to $\delta(t - t')$ are due to the incoming vacuum field reflected by the coupling mirror of the cavity. The second terms are related to the fields coming out of the cavity. For individual pulses, i.e. when $n = n'$, one can neglect second terms which are proportional to $\kappa_s T_R \ll 1$. Thus the fluctuations of the quadratures in the pulses are vacuum fluctuations, except the fluctuations of X-quadrature which become infinitely large close to threshold when $\mu_0 \to 1$. Since these solutions are obtained under the assumption of small fluctuations one must define how close can we approach the threshold from above. It is shown in the Appendix C that for typical experimental parameters the condition of small fluctuations is fulfilled and the solutions are correct if $(\mu_0 - 1) \gg 10^{-3}$. Therefore we will use the following minimal value of the pump parameter in quantitative estimations $\mu_0 = 1.1$.

There are also quantum correlations between different pulses (when $n \neq n'$) for the X- quadrature of the fields, and anticorrelations for the Y-quadrature with the correlation coefficient proportional to $\kappa_s T_R$. The number of significantly correlated successive pulses can be evaluated by the factor in the exponential, which is proportional to $(\kappa_s T_R)^{-1}$. The delta-function shows that the correlations between different pulses have a "local" character: they are effective only when the time differences are a multiple of the period T_R.

Correlation coefficient and number of correlated pulses also depend on pump parameter μ_0 (i.e. on pump power). For Y-quadrature of the signal field they are maximal close to threshold, when $\mu_0 \approx 1$. For Y-quadrature of the pumping field correlation coefficient tends to zero in the vicinity of threshold. Away from threshold the correlation increases while the number of correlated pulses decreases. Also close to threshold the fluctuations of the X-quadrature of signal field becomes infinitely large, which restricts the minimal value of pump parameter as remarked above.

Solutions (23) and (24) also show that fluctuations of pump and signal fields are correlated in contrast to below threshold regime. One can get the following symmetrized cross-correlation functions for these fields at the output of the oscillator

$$\begin{aligned} &\langle \delta\hat{X}_{p,n}^{out}(t - nT_R)\delta\hat{X}_{s,n'}^{out}(t' - n'T_R)\rangle + \langle \delta\hat{X}_{s,n}^{out}(t - nT_R)\delta\hat{X}_{p,n'}^{out}(t' - n'T_R)\rangle = \\ &\qquad - \kappa_s T_R\sqrt{\frac{1}{2(\mu_0 - 1)}}\, e^{-2\kappa_s T_R(\mu_0 - 1)|n-n'|}\delta(t - t' - (n-n')T_R), \end{aligned} \tag{31}$$

$$\begin{aligned} &\langle \delta\hat{Y}_{p,n}^{out}(t - nT_R)\delta\hat{Y}_{s,n'}^{out}(t' - n'T_R)\rangle + \langle \delta\hat{Y}_{s,n}^{out}(t - nT_R)\delta\hat{Y}_{p,n'}^{out}(t' - n'T_R)\rangle = \\ &\qquad - \kappa_s T_R\sqrt{\frac{(\mu_0 - 1)}{2\mu_0^2}} e^{-2\kappa_s T_R\mu_0|n-n'|}\delta(t - t' - (n-n')T_R) \end{aligned} \tag{32}$$

The properties of the cross-correlations (number of correlated pulses, correlation coefficient and local character of correlations) are analogous to the properties of fields itself that we have considered above. Close to the oscillation threshold the correlations between pump and signal fields become infinitely large for X-quadrature and decrease for Y-quadrature. The minus sign indicates that the fluctuations are anti-correlated.

VI. QUANTUM EFFECTS IN THE SPECTRA OF FIELDS

Let us remind that the temporal features associated with the correlations of pulses are small (of the order of $\kappa_s T_R \ll 1$), while the number of correlated pulses is defined by inverse value $(\kappa_s T_R)^{-1}$. Therefore one expects to obtain important quantum effects by observing integral characteristic of fields, such as the Fourier spectrum of fluctuations of quadratures. Let us consider the measurement of field quadratures obtained by a balanced homodyne detection of the output fields (see Fig. 3). The signal or pump field is mixed at a symmetric beamsplitter with an intense local oscillator field of the same optical frequency ($\omega_p/2$ or ω_p). In this case the fluctuations of the difference photocurrent are given by the expression

$$\delta\hat{i}_r(t) = \beta^*(t)\, \delta\hat{A}_r^{out}(t) + \beta(t)\, \delta\hat{A}_r^{out\dagger}(t), \tag{33}$$

where $\beta(t)$ is the complex amplitude of the local oscillator. We suppose here that the local oscillator field is a train of identical pulses and that their period is equal to the period of analyzed pulses T_R

$$\beta(t) = \sum_n \beta_0(t - nT_R). \tag{34}$$

The envelope of pulses has the form

$$\beta_0(t) = \sqrt{N_{LO}(t)}\, e^{i(\varphi(t)+\Phi)}, \tag{35}$$

where phase modulation of pulses is matched with the detected field: for pump field $\varphi(t) = \phi_{in}(t)$, for signal field $\varphi(t) = \phi_{in}(t)/2$. As a result choosing constant phase shift $\Phi = 0$ or $\Phi = \pi/2$ one finds:

$$\delta\hat{i}_r(t) = 2\sum_n \sqrt{N_{LO}(t_n)} \begin{pmatrix} \delta\hat{X}_{r,n}^{out}(t_n) \\ \\ \delta\hat{Y}_{r,n}^{out}(t_n) \end{pmatrix}, \qquad t_n = t - nT_R. \tag{36}$$

The shape of local oscillator pulses, their duration and delay relative to the pulses of the fields to analyze can be experimentally adjusted. We suppose here that the pulses have a rectangular shape of duration τ_p and are ideally synchronized with the pulses of analyzed field. In this case the current fluctuations are equal to the quantum fluctuations of the fields inside pulses. In Sec. VII we will generalize our results to arbitrary envelopes of pump and local oscillator pulses.

Let us now consider the measurement of Y-quadratures of pump and signal fields. Substituting expressions (28) and (30) in (36), we derive the pair correlation functions for the currents:

$$\langle \delta\hat{i}(t)\, \delta\hat{i}(t')\rangle_p = \sum_n N_{LO}(t - nT_R) \left(\delta(t-t') - 2\kappa_s T_R \frac{(\mu_0 - 1)}{\mu_0} e^{-2\kappa_s\mu_0|t-t'|} \sum_{n'} \delta\left(t - t' - (n-n')T_R\right) \right), \tag{37}$$

$$\langle \delta\hat{i}(t)\, \delta\hat{i}(t')\rangle_s = \sum_n N_{LO}(t - nT_R) \left(\delta(t-t') - \frac{\kappa_s T_R}{\mu_0} e^{-2\kappa_s\mu_0|t-t'|} \sum_{n'} \delta\left(t - t' - (n-n')T_R\right) \right). \tag{38}$$

One sees that the correlations between pulses lead to temporal periodic correlations of the photocurrent. Let us determine the frequency spectrum of the photocurrent quantum noise defined as:

$$\left(\delta i^2\right)_\Omega = \lim_{T\to\infty} \frac{1}{T} \int_{-T/2}^{+T/2} dt \int_{-T/2}^{+T/2} dt'\, \langle \delta\hat{i}(t)\, \delta\hat{i}(t')\rangle\, e^{i\Omega(t-t')} \tag{39}$$

Substituting (37) and (38) into (39) one gets the following explicit expressions for the spectrum of the detected pump field

$$\frac{(\delta i_p^2)_\Omega}{\langle I\rangle} = 1 - \sum_{m=0,1,2...} \frac{8\kappa_s^2(\mu_0 - 1)}{4\kappa_s^2\mu_0^2 + (\Omega - 2\pi m/T_R)^2}, \tag{40}$$

and signal field

$$\frac{(\delta i_s^2)_\Omega}{\langle I\rangle} = 1 - \sum_{m=0,1,2...} \frac{4\kappa_s^2}{4\kappa_s^2\mu_0^2 + (\Omega - 2\pi m/T_R)^2}. \tag{41}$$

Here fluctuations are normalized to the corresponding shot (quantum) noise of local oscillator

$$\langle I\rangle = \frac{1}{T_R}\int_{-T_R/2}^{+T_R/2} dt\, N_{LO}(t), \tag{42}$$

which for rectangular pulses is equal to $\langle I\rangle = (\tau_p/T_R)N_{LO}$.

These expressions show that the shot noise is reduced around all resonant frequencies of the cavity $\Omega_m = 2\pi m/T_R$. This coincides with the result obtained in the below threshold regime. For pump field a maximal noise reduction of fifty percent is achieved at $\mu_0 = 2$. For signal field the expression predicts full reduction of the noise at the oscillation threshold, i.e. $(\delta i_s^2)_{\Omega_m}/\langle I\rangle \to 0$ when $\mu_0 \to 1$.

VII. ARBITRARY SHAPES OF PULSES

Our results can be easily generalized to arbitrary shapes of pump pulses with corresponding pump parameter $\mu(t)$. This is possible because in our model different temporal parts of individual pulses develop independently of each other inside SPOPO. Hence at time instants when instantaneous pump power exceeds parametric threshold, i.e. $\mu(t) > 1$, the average amplitude and fluctuations of signal field are defined by (7)-(8) and (29)-(30), respectively, where replacement $\mu_0 \to \mu(t)$ is made. The average amplitude of intracavity pump field is stabilized at the threshold value according to (7)-(8) and its fluctuations are characterized by correlations (27) and (28). At other time instants, when $\mu(t) < 1$, the signal field is in the below threshold regime.

Also it is not difficult to generalize the results of balanced homodyne detection, namely the spectra (40) and (41), that we have derived for rectangular pump and local oscillator pulses. Let us assume that the local oscillator pulses with the envelope $N_{LO}(t)$ are quite short ($\tau_{LO} < \tau_p$) and synchronized with the analyzed pulses to probe temporal parts of the pulses generated above threshold. Then general expressions can be obtained by averaging intensity shape of the local oscillator pulses with expressions (40) and (41), where pump parameter depends on time $\mu(t)$

$$(\delta i_p^2)_\Omega = \frac{1}{T_R}\int_{-T_R/2}^{+T_R/2} dt\, N_{LO}(t)\left(1 - \sum_{m=0,1,2...} \frac{8\kappa_s^2(\mu(t)-1)}{4\kappa_s^2\mu^2(t) + (\Omega - 2\pi m/T_R)^2}\right), \tag{43}$$

$$(\delta i_s^2)_\Omega = \frac{1}{T_R}\int_{-T_R/2}^{+T_R/2} dt\, N_{LO}(t)\left(1 - \sum_{m=0,1,2...} \frac{4\kappa_s^2}{4\kappa_s^2\mu^2(t) + (\Omega - 2\pi m/T_R)^2}\right). \tag{44}$$

These expressions mean that current fluctuations at a particular frequency appear as a weighted sum (integral) of fluctuations from all non-correlated parts of the measured pulses. Consequently, the detected quantum noise is sensitive to the temporal properties of the local oscillator pulses, particularly to their duration and to the delay relative to analyzed pulses, as in the below threshold regime. Fig. 4 presents suppression of the photocurrent shot noise at zero frequency as a function of delay Δt of short local oscillator pulses ($\tau_{LO} \ll \tau_p$) relative to the signal ones. Curves are obtained for Gaussian pump pulses of SPOPO $\mu(t) = \mu_0 e^{-2(t/\tau_p)^2}$ and with different values of peak power, including below threshold values. In order to determine the noise suppression at the edges of the signal pulses, where the field is in the below threshold regime, we used the following expression of the photocurrent spectrum from [9]

$$\left(\delta i_s^2\right)_\Omega^{below} = \frac{1}{T_R}\int_{-T_R/2}^{+T_R/2} dt N_{LO}(t)\left(1 - \sum_{m=0,1,2,...} \frac{4\kappa_s^2\mu(t)}{\kappa_s^2\left(1+\mu(t)\right)^2 + (\Omega - 2\pi m/T_R)^2}\right). \tag{45}$$

This expression was also used in the case when the peak pump power is less than the threshold value, i.e. $\mu_0 < 1$.

The figure shows that the fluctuations of signal field are nonuniform inside pulses. In the central part of bright pulses ($\mu_0 > 1$), where the field intensity is maximal, the fluctuations are larger than at the edges. Of course measuring local squeezing with the help of infinitely short LO pulses is a purely theoretical scheme. In the realistic case when pulses of local oscillator have finite duration, the photocurrent fluctuations must be weighted by the intensity of the local oscillator pulse that corresponds to expression (44).

VIII. CONCLUSION

Let us summarize our results: if the peak pump power exceeds the threshold of continuous OPO oscillation then both regimes (below and above threshold) coexist at different times within the pulses of signal field. Bright parts of the pulses above threshold are characterized by an average amplitude. At the edges of pulses the field has properties of the below threshold case. The quantum fluctuations of pulses turn out to be totally not correlated at different times within the same pulse, whereas they are correlated between nearby pulses at times that are placed in the same position relative to the center of the pulses. Above threshold the model also predicts the existence of correlations between pump pulses with the same properties and cross-correlations between pump and signal pulses.

These correlations can be measured in the scheme of balanced homodyne detection using a pulsed local oscillator synchronized with the required times of the analyzed field. We have also shown that these correlations lead to a suppression of quantum noise in the spectra of phase quadratures of pump and signal fields around frequencies $\Omega_m = 2\pi m/T_R$ $(m = 0, 1, 2, \ldots)$, where T_R period of pulses. A stronger noise suppression is achieved under detection of signal field when thelocal oscillator pulses are delayed relative to the peak of signal ones.

Since a SPOPO is a multimode system it is interesting to compare our results with the prediction of the paper [11]. According to this paper, when one increases the pump power, the multimode parametric oscillator starts oscillating in the mode with the lowest oscillation threshold whereas other modes stay in non-critically squeezed vacuum states.

One can consider for SPOPO that the bright parts of the signal pulses correspond to the modes developing above threshold and the field at the edges of pulses is formed by the below threshold modes. The correlation properties of the field show that an individual mode is a train of correlated delta pulses whereas different modes appear as trains of pulses delayed to each other.

It is well-known that the balanced homodyne detection technique detects optical field amplitudes in a particular spatial-temporal mode defined by a coherent local oscillator pulse [14]. Therefore shot noise suppression at the Fig. 4 could be treated as a squeezing of the stated modes of signal field since different delays of the local oscillator correspond to the detection of different modes. Further interpretation of the results in terms of the modes apparently should take into account dispersion effects in the parametric crystal such as mismatch and dispersion of group velocities.

The study was performed within the framework of the Russian- French Cooperation Program "Lasers and Advanced Optical Information Technologies" and the European Project HIDEAS (grant No. 221906). It was also supported by RFBR (No. 08-02-92504).

[1] W. Wasilewski, A. I. Lvovsky, K. Banaszek, and C. Radzewicz, “Pulsed squeezed light: Simultaneous squeezing of multiple modes,” *Phys. Rev. A*, vol. 73, p. 063819, Jun 2006.

[2] M. Lassen, V. Delaubert, J. Janousek, K. Wagner, H.-A. Bachor, P. K. Lam, N. Treps, P. Buchhave, C. Fabre, and C. C. Harb, “Tools for multimode quantum information: Modulation, detection, and spatial quantum correlations,” *Phys. Rev. Lett.*, vol. 98, p. 083602, Feb 2007.

[3] B. Chalopin, G. Patera, G. de Valcárcel, N. Treps, and C. Fabre, “Multimode opos as sources for multipartite entanglement,” in *Conference on Lasers and Electro-Optics/International Quantum Electronics Conference*, p. IThK2, Optical Society of America, 2009.

[4] G. Leuchs and D. Bruss, eds., *Lectures on Quantum Information.* VCH Verlagsgesellschaft mbH, 2007.

[5] N. C. Menicucci, S. T. Flammia, and O. Pfister, “One-way quantum computing in the optical frequency comb,” *Phys. Rev. Lett.*, vol. 101, p. 130501, Sep 2008.

[6] H. M. van Driel, “Synchronously pumped optical parametric oscillators,” *Applied Physics B: Lasers and Optics*, vol. 60, pp. 411–420, 1995. 10.1007/BF01081320.

[7] G. J. de Valcárcel, G. Patera, N. Treps, and C. Fabre, “Multimode squeezing of frequency combs,” *Phys. Rev. A*, vol. 74, p. 061801, Dec 2006.

[8] G. Patera, N. Treps, C. Fabre, and G. J. de Valcárcel, “Quantum theory of synchronously pumped type i optical parametric oscillators: characterization of the squeezed supermodes,” *Eur. Phys. J. D*, vol. 56, no. 1, pp. 123–140, 2010.

[9] V. A. Averchenko, Y. M. Golubev, C. Fabre, and N. Treps, “Quantum correlations and fluctuations in the pulsed light produced by a synchronously pumped optical parametric oscillator below its oscillation threshold,” *Eur. Phys. J. D*, vol. 61, no. 1, pp. 207–214, 2011.

[10] D. F. Walls and G. J. Milburn, *Quantum Optics.* Springer, 1995.

[11] B. Chalopin, F. Scazza, C. Fabre, and N. Treps, “Multimode nonclassical light generation through the optical-parametric-oscillator threshold,” *Phys. Rev. A*, vol. 81, p. 061804, Jun 2010.

[12] M. A. M. Marte, H. Ritsch, K. Petsas, A. Gatti, L. Lugiato, C. Fabre, and D. Leduc, “Spatial patterns in optical parametric oscillators with spherical mirrors: classical and quantum effects,” *Opt. Express*, vol. 3, pp. 71–80, Jul 1998.

[13] F. Zernike and J. E. Midwinter, *Applied Nonlinear Optics.* Dover Publications, 2 ed., 2006.

[14] M. G. Raymer, P. D. Drummond, and S. J. Carter, "Limits to wideband pulsed squeezing in a traveling-wave parametric amplifier with group-velocity dispersion," *Opt. Lett.*, vol. 16, pp. 1189–1191, Aug 1991.
[15] M. I. Kolobov, "The spatial behavior of nonclassical light," *Rev. Mod. Phys.*, vol. 71, pp. 1539–1589, Oct 1999.
[16] F. Rana, R. J. Ram, and H. A. Haus, "Quantum Noise of Actively Mode-Locked Lasers With Dispersion and Amplitude/Phase Modulation," *IEEE Journal of Quantum Electronics*, vol. 40, pp. 41–56, Jan. 2004.

Appendix A

In the degenerate parametric generation configuration that we consider here the field operator inside the cavity is equal to

$$\hat{E}(z,t) = \hat{E}_p(z,t) + \hat{E}_s(z,t). \tag{A1}$$

We use the plane wave approximation, so that the field amplitudes depend only on one longitudinal coordinate z measured along optical axis of the cavity. As the pump of the parametric crystal is realized by a train of optical pulses of duration close to $100fs$ it is possible to disjoint in the standard form quick oscillations of fields with optical frequencies $\omega_{p,s}$ from slow changes of their envelopes [15]. At the crystal entrance ($z=0$) for the pump p and signal s waves the two fields read

$$\hat{E}_r(0,t) = i\left(\frac{\hbar\omega_r}{2n_r\varepsilon_0 cS}\right)^{1/2} e^{-i\omega_r t}\,\hat{A}_r(0,t), \qquad r = s,p, \qquad (\omega_p = 2\omega_s), \tag{A2}$$

where $n_r = n_r(\omega_r)$ are the indices of refraction of the crystal. Following expression takes into account the periodic temporal structure of the fields

$$\hat{A}_r(0,t) = \sum_n \hat{A}_{r,n}(t - nT_R). \tag{A3}$$

Here $\hat{A}_{r,n}(t-nT_R)$ is the envelope of the n-th pulse. Argument of the envelope $t-nT_R$ describes time deviation from the pulse center and changes in the interval from $-T_R/2$ to $T_R/2$.

In order to describe evolution of fields inside the SPOPO cavity we use the two-time approach applied by Haus in Ref. [16] for developing a quantum theory of actively mode-locked lasers. We assume that the envelopes of pulses are not significantly changed from one pulse to the next, an hypothesis that is typically valid in experiments with high-finesse cavity and weak parametric amplification. Then the dependence on discrete number n could be replaced approximately by the a continuously varying temporal parameter T in the following way

$$\hat{A}_{r,n}(t - nT_R) \to \hat{A}_r(t,T), \tag{A4}$$

where t on the right hand side of the expression denotes time deviation from the pulse center. Thus expressions (A3) and (A4) esteblish correspondence between envelope of the field $\hat{A}_r(0,t)$ and envelope of an individual pulse $\hat{A}_r(t,T)$ that depends on two time parameters.

Appendix B

Let us determine properties of Langevine noise sources entering in the Heisenberg-Langevine equations (1) and (2). The sources are caused by vacuum fluctuations of incoming coherent/vacuum fields. Following expression directly connects these quantities

$$\hat{F}_r(t) = \frac{\sqrt{\mathcal{T}_r}}{T_R}\hat{A}_r^{vac}(t) \approx \sqrt{\frac{2\kappa_r}{T_R}}\hat{A}_r^{vac}(t), \qquad r = s,p, \tag{B1}$$

where $\mathcal{T}_r$ is the transmission coefficient of the mirror at the corresponding frequency. Vacuum fluctuations are characterized by the following non-zero correlation functions

$$\langle \hat{A}_r^{vac}(t)\hat{A}_r^{vac\,\dagger}(t')\rangle = \delta(t-t'). \tag{B2}$$

Using written expressions and pulse representation of slow envelopes (A3) one gets that noise terms should satisfy following relations

$$\langle \hat{F}_{r,n}(t-nT_R)\hat{F}^{\dagger}_{r,n'}(t'-n'T_R)\rangle = \frac{2\kappa_r}{T_R}\delta_{nn'}\delta(t-nT_R-(t'-n'T_R)). \tag{B3}$$

Finally making transition to continuous time parameter (A4) and using relations $\delta_{nn'} \to T_R\delta(T-T')$ and $t-nT_R \to t$, one gets required correlators (4).

Appendix C

Here we determine values of pump parameter at which the condition of small fluctuations is fulfilled: $\delta\hat{A}_r(t,T) \ll \sqrt{N_r}$. It was shown in Sec. V that above threshold fluctuations of fields are vacuum except X-quadrature of signal field whose fluctuations become infinitely large in the vicinity of threshold when $\mu_0 \to 1$. Therefore condition of small fluctuations could be written in the form

$$\langle \delta\hat{X}_s^2 \rangle \ll N_s, \tag{C1}$$

where $\langle \delta\hat{X}_s^2 \rangle$ is a variance of X-quadrature of intracavity signal field. In order to determine it let us evaluate correlation function of the quadrature $\langle \delta\hat{X}_s(t,T)\ \delta\hat{X}_s(t',T') \rangle$. The function could be easily obtained using explicit expression for fluctuations of X-quadrature (24) and correlation functions for Langevine noise sources (21). One gets

$$\langle \delta\hat{X}_s(t,T)\ \delta\hat{X}_s(t',T') \rangle = \frac{1}{4}\left(1 + \frac{1}{2(\mu_0 - 1)}\right) e^{-2\kappa_s(\mu_0-1)(T-T')}\delta(t-t') \tag{C2}$$

We have to put $T = T'$ and $t = t'$ in the expression in order to find quadrature variance. However divergence appears due to the fact that field fluctuations are not correlated in each individual pulse. One can avoid the difficulty defining dispersion in the following way

$$\langle \delta\hat{X}_s^2 \rangle = \frac{1}{T_F} \int\limits_{t-T_F/2}^{t+T_F/2} dt'\ \langle \delta\hat{X}_s(t,T)\ \delta\hat{X}_s(t',T) \rangle \tag{C3}$$

where T_F is an averaging time. Thus dispersion is given by

$$\langle \delta\hat{X}_s^2 \rangle = \frac{1}{T_F} \cdot \frac{1}{4}\left(1 + \frac{1}{2(\mu_0 - 1)}\right) \tag{C4}$$

Finally let us take into account that average classical intensity of signal field tends to zero in the vicinity of threshold according to expression $N_s = \frac{2\kappa_p}{\kappa_s}(\mu_0 - 1)N_{th}$. Therefore the condition of small fluctuations is fulfilled if:

$$\mu_0 - 1 \gg \sqrt{\frac{\kappa_s}{\kappa_p}\,\frac{1}{N_{th}T_F}} \tag{C5}$$

In order to estimate this restriction let us choose following parameters [8]: pump wavelength $\lambda_p = 0.4\mu$m, threshold power of continuous generation $P_{th} = 50$W, averaging time (which is equal to the correlation time) $T_F = 10$fs and $\kappa_p = 10\kappa_s$. As a result one gets

$$\mu_0 - 1 \gg 10^{-3}. \tag{C6}$$

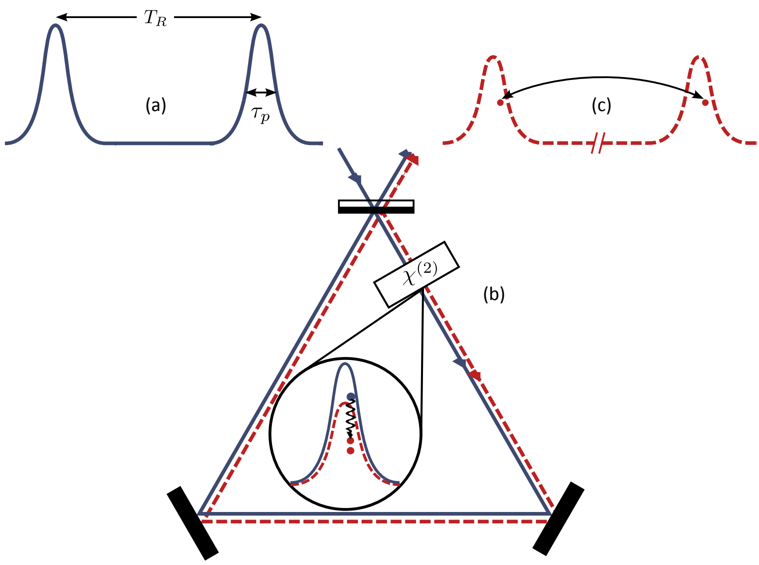

FIG. 1: Synchronously pumped optical parametric oscillator (SPOPO): (a) pulsed pumping field; (b) parametric down-conversion of pump photon in a pair of signal photons inside a nonlinear crystal; (c) establishing of quantum correlations between pulses of output signal field. Solid line - pump field; dashed line - signal field.

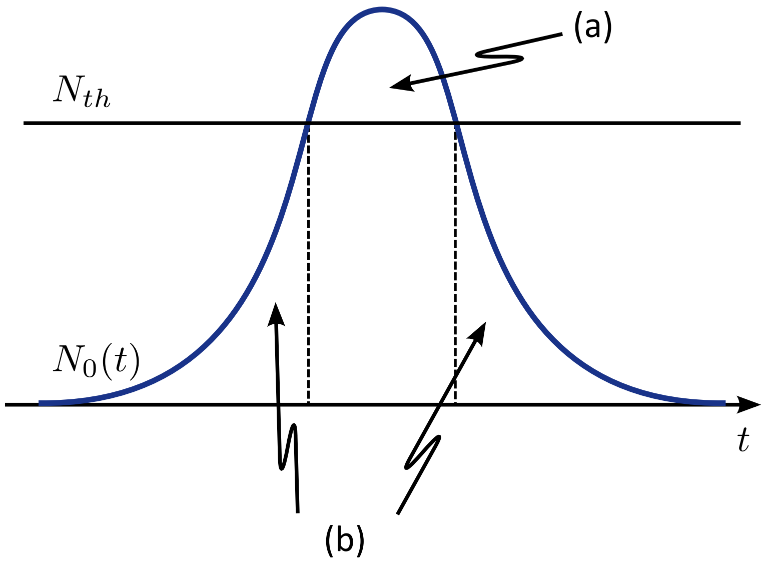

FIG. 2: Two regimes of oscillation within an individual pump pulse of SPOPO: (a) above threshold regime; (b) below threshold regime. N_{th} - threshold power of continuous generation; $N_0(t)$ - instantaneous power of pulsed pumping.

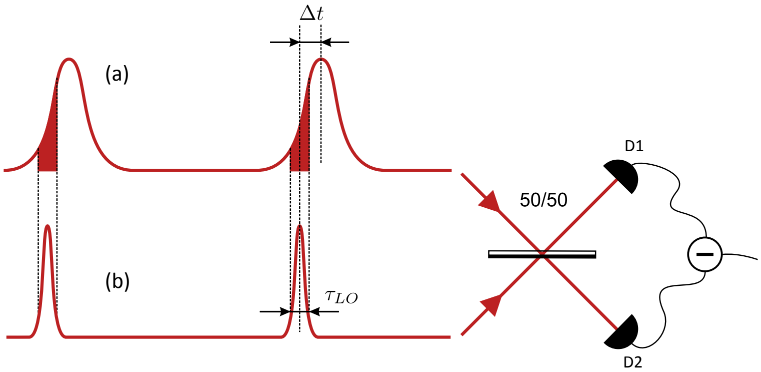

FIG. 3: Balanced homodyne detection of a pulsed field: (a) analyzed field; (b) local oscillator. The parameters that can be changed in the setup are the duration of the local oscillator pulses τ_{LO} and their delay Δt relative to the signal pulses.

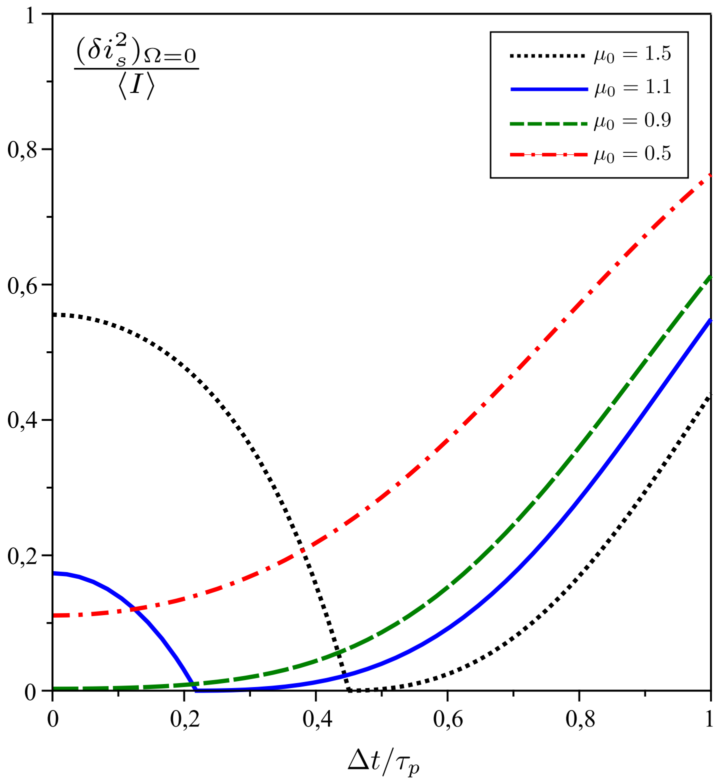

FIG. 4: Shot noise reduction of difference photocurrent at zero frequency in dependence of delay Δt of short local oscillator pulses ($\tau_{LO} \ll \tau_p$) relative to signal ones. Pump pulses are Gaussian with different values of peak power μ_0.